Bare PCB Inspection System With SV-GMR Sensor Eddy-Current Testing Probe

Bare PCB Inspection System With SV-GMR Sensor Eddy-Current Testing Probe

Komkrit Chomsuwan, *Member, IEEE,* Sotoshi Yamada, *Member, IEEE,* and Masayoshi Iwahara, *Member, IEEE*

Abstract—This paper describes bare printed circuit board (PCB) inspection based on eddy-current testing (ECT) technique with high scanning speed. A high-frequency ECT probe composed of a meander coil as an exciting coil and the spin-valve giant magnetoresistance (SV-GMR) sensor was fabricated and is proposed. The ECT probe was designed based on crack inspection over flat surface, especially suitable for microdefect detection on high-density bare PCB. The ECT signal detected by the SV-GMR sensor was acquired by high-speed A/D converter for applying the signal processing based on digital technique. Harmonic analysis based on Fourier transform was used to analyze the ECT signal at fundamental frequency in order to increase inspection speed and this technique allowed the ECT probe to scan bare PCB, with high sampling frequency and with high-spatial resolution inspection. Experimental results verified the possibility and the performance of the proposed PCB inspection system based on ECT technique.

Index Terms—Eddy-current testing (ECT), harmonic analysis, inspection, printed circuit board (PCB), spin-valve giant magnetoresistance (SV-GMR).

I. INTRODUCTION

INSPECTION of a high-density bare printed circuit board (PCB) requires an accurate inspection system to reduce the PCB assemble cost. Normally, the identification of the defects on the PCB conductor is very difficult because there have many kinds of defects, for example, disconnection, short circuit, potential defect, misplacement, etc., that need to be inspected, therefore many processes of PCB inspection are required. PCB defect detection procedures can be broadly divided into two classes: contact method or electrical test and noncontact method or nonelectrical test [1]. For electrical test, it provides the information of conductor disconnection, short circuit, and a test of functionality of a board. Although many parameters can be successfully checked by electrical test, it has limitations that could allow defective products to pass. Potential defects such as line width or spacing reductions are not detected. Automatic visual/optical inspection is well-known and widely used for PCB inspection because this technique provides high throughput and is inexpensive. Track width error and misplacements can be detected by the automation visual/optical inspection. However, this technique is limited to inspect only on the outer surface of the PCB. Therefore, it is difficult to examine very small defects occurring on the coated PCB conductor.

The eddy-current testing (ECT) technique is the well-known method of nondestructive evaluation technique that is, usually, applied to evaluate the material flaws without changing or altering of testing material. The advantage of the ECT technique is highly sensitive to material conductivity which depends on many variables such as material thickness, crack, etc. Therefore, the ECT technique is usually used to detect dangerous cracks on aircraft, such as around fastener holes and jet engines, and it is also used to inspect microcracks in nuclear power plant equipment, such as reactors, turbines, and the pipeline systems [2], [3].

Bare PCB inspection system based on the ECT technique has been developed and is successfully applied to detect microdefects on microconductors of bare PCB [4], [5]. Moreover, this technique can be applied in inspecting the dimension and alignment of the PCB conductor [6]. The construction of the ECT probe consists only of an exciting coil and magnetic sensor; therefore, it is cost effective and very simple to fabricate. Although there are several kinds of magnetic sensors, such as hall, superconducting quantum interference device (SQUID), planar mesh-type, etc., they have been successfully applied to the ECT technique in the detecting material cracks and properties. The giant magnetoresistance (GMR) sensor is very interesting and it is possible to apply it to high-density PCB inspection based on the ECT technique [7]–[9]. A spin-valve giant magnetoresistance (SV-GMR) device is selected to be used as a magnetic sensor because it has high sensitivity and high resolution, ranging from nanotesla to several millitesla, and provides good performance versus its cost. Furthermore, it can operate at a high-frequency magnetic field and has high-spatial resolution [10]. However, the ECT signal obtained from the SV-GMR sensor is low; thus, a high-performance measurement technique is required to improve signal-to-noise ratio (SNR). Phase-sensitive detection, well-known as lock-in amplifier, is one of the measurement techniques, which can improve SNR more than 60 dB [11]. However, the inspection speed and spatial resolution of inspection are restricted by the utilization of the lock-in amplifier. For the application to PCB manufacturing process, the scanning speed and spatial resolution of inspection have to
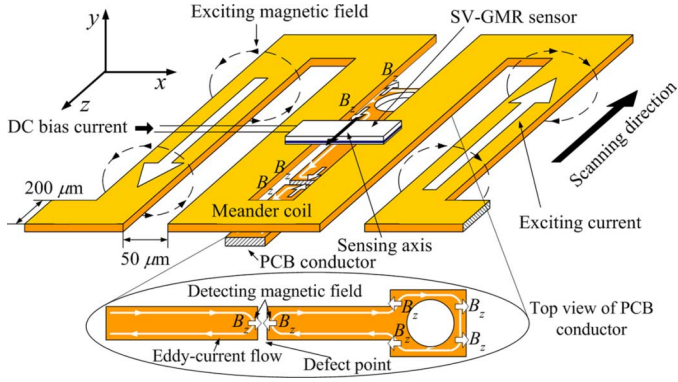
Fig. 1. Proposed SV-GMR sensor ECT probe.

Fig. 2. Picture of proposed SV-GMR sensor.

be improved for providing high-inspection throughput and accurate inspection results.

In this paper, high-frequency ECT probe structure and its inspection system were proposed. The ECT probe was designed based on a high-frequency ECT probe and applied to flat surface inspection that was suited to high-density bare PCB inspection. The increasing of the scanning speed and spatial resolution of bare PCB inspection with ECT technique by application of harmonic analysis based on Fourier transform was proposed. Fourier transform was used to analyze the ECT signal obtained from the SV-GMR sensor. SNR acquired by the harmonic analysis technique was studied. Inspection of the simple PCB model also shows the possibility of the proposed technique for PCB inspection application.

II. PROPOSED ECT SYSTEM STRUCTURE

A. ECT Probe Construction

As shown in Fig. 1, the proposed high-frequency ECT probe structure, which consisted of a long meander coil and the SV-GMR device serving as an exciting coil and a magnetic sensor, respectively, was fabricated for the high-density bare PCB inspection. The SV-GMR sensor was mounted on the long meander coil and its sensing axis was set to detect the magnetic field, B_z, only in the scanning direction that usually occurs at defect point or at PCB conductor boundary. The use of the long meander coil provides the advantage of easily developing the multisensor, which is another technique that can improve the scanning speed [12], [13]. In addition, it provides a short distance between the SV-GMR sensor and tested PCB. As a result, the SV-GMR sensor easily acquires the ECT signal at defect point with high SNR.

The SV-GMR sensor, with a sensing area of $93\,\mu m \times 100\,\mu m$, had the structure and small signal characteristics, as shown in Figs. 2 and 3, respectively. Normal resistance of the SV-GMR sensor was approximately $400\,\Omega$, while it had maximum MR ratio approximately of 12% of normal resistance or it had maximum resistance variation between 370 and $420\,\Omega$. Furthermore, its sensitivity in sensing direction, the B_z axis, was approximately $150\,\mu V/\mu T$, while it was lower than $15\,\mu V/\mu T$ in the other axes, B_x and B_y, when bias current of 5 mA was applied.
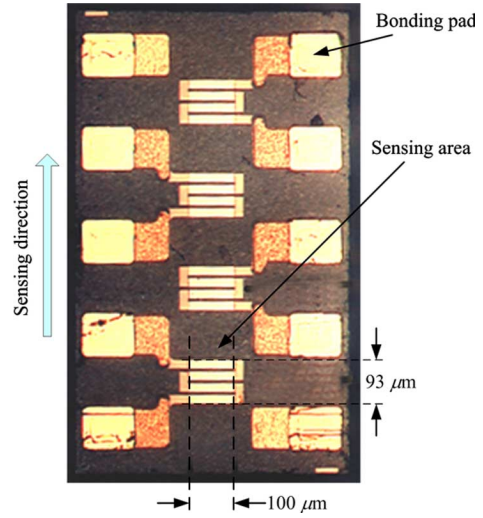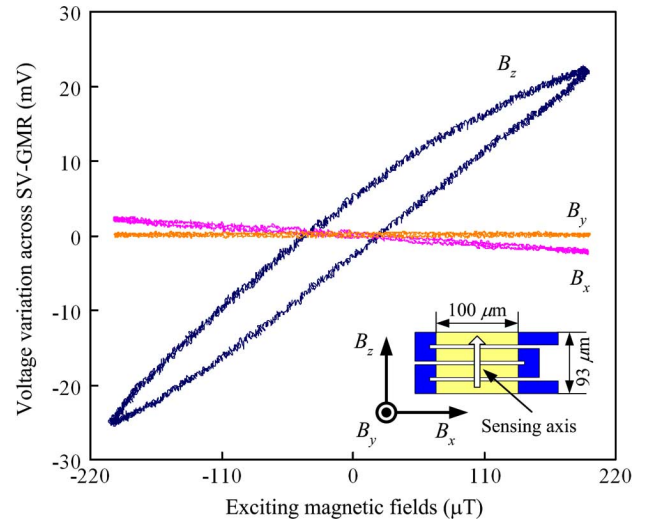

Fig. 3. Small signal characteristics of the SV-GMR sensor.

B. System Structure

The proposed system structure consisted of four parts, as shown in Fig. 4. The first was the PCB position control system for moving the tested PCB in two dimensions. The second was the aforementioned high-frequency ECT probe. The third was the exciting system. Magnetic field excitation was generated by feeding high-frequency exciting current to the long meander coil. In this research, sinusoidal current of 200 mA at a frequency of 5 MHz was fed to the meander coil. Finally, the forth was the data acquisition system that, normally, used the lock-in amplifier for measuring the ECT signal from the SV-GMR sensor. For decreasing inspection time, a high-speed A/D converter (12 bits at sampling frequency of 100 MS/s) was used to capture the ECT signal from the SV-GMR sensor and transferred the data to the computer. Harmonic analysis based on Fourier transform implemented with digital technique was applied to the captured signal. Then, the PCB inspection with high-speed scanning produced the inspection resulting in less distortion.
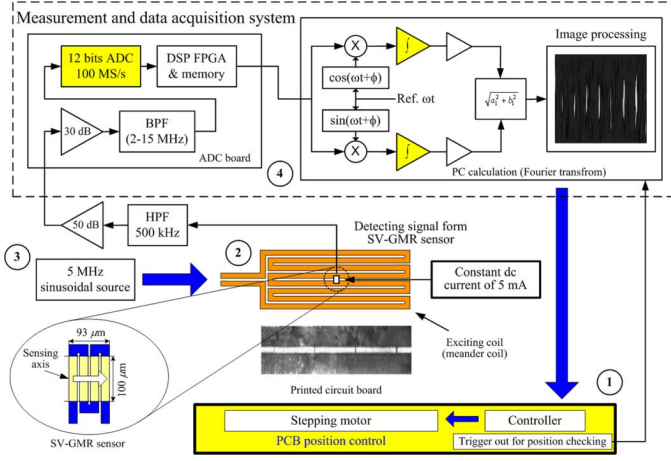
Fig. 4. PCB inspection system based on ECT technique.

Fig. 5. Effect of the number of samples of captured signal, m, per spatial sample to noise reduction.

III. MEASUREMENT SYSTEM

The noisy input signal $v_{\text{in}}(t)$ measured from the SV-GMR sensor can be written with the signal and noise terms as follows:

$$v_{\text{in}}(t) = V_s \sin(\omega t + \theta_s)$$
$$+ \sum_{\text{noise}=1}^{\infty} [V_{\text{noise}} \sin(\omega_{\text{noise}} t + \theta_{\text{noise}})] \quad (1)$$

where V_s, ω, and θ_s are amplitude, fundamental frequency, and phase shift of the signal, respectively, and $V_{\text{noise}}, \omega_{\text{noise}}$, and θ_{noise} are amplitude, frequency, and phase shift of the noise, respectively.

To measure the signal at fundamental frequency, the measured signal $v_{\text{in}}(t)$ in (1) is multiplied by cosine and sine function at the fundamental frequency. Therefore, the multiplying signal V_x, multiplied with cosine function, and V_y, multiplied with sine function, can be obtained as follows:

$$V_x = (V_s/2)\sin(\theta_s - \theta_r) + (V_s/2)\sin(2\omega t + \theta_s + \theta_r)$$
$$+ \sum_{\text{noise}=1}^{\infty} \{(V_{\text{noise}}/2)\sin[(\omega_{\text{noise}} - \omega)t + \theta_{\text{noise}} - \theta_r]\}$$
$$+ \sum_{\text{noise}=1}^{\infty} \{(V_{\text{noise}}/2)\sin[(\omega_{\text{noise}} + \omega)t + \theta_{\text{noise}} + \theta_r]\}$$
$$(2)$$

$$V_y = (V_s/2)\cos(\theta_s - \theta_r) + (V_s/2)\cos(2\omega t + \theta_s + \theta_r)$$
$$+ \sum_{\text{noise}=1}^{\infty} \{(V_{\text{noise}}/2)\cos[(\omega_{\text{noise}} - \omega)t + \theta_{\text{noise}} - \theta_r]\}$$
$$- \sum_{\text{noise}=1}^{\infty} \{(V_{\text{noise}}/2)\cos[(\omega_{\text{noise}} + \omega)t + \theta_{\text{noise}} + \theta_r]\}$$
$$(3)$$

where θ_r is phase shift of the multiplying function.

In case of the lock-in amplifier, a low-pass filter was applied to (2) and (3) to obtain only a dc component, $(V_s/2)\sin(\theta_s - \theta_r)$ and $(V_s/2)\cos(\theta_s - \theta_r)$. Whenever the low frequency term, $(\omega_{\text{noise}} - \omega)$, approaches dc, cutoff frequency of the low-pass filter had to approach dc. As a result, the time constant τ was high and, therefore, to measure the signal, the measurement had
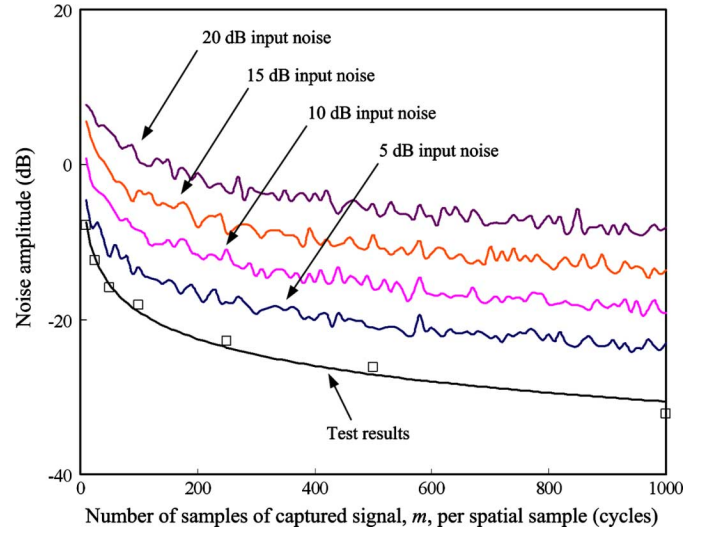
to be delayed until obtaining the signal at steady-state value. It means that the measurement time at each spatial sample depended on the time constant, τ, thus, the scanning speed was restricted. To eliminate this effect, instead of using low-pass filter, integration within interval time t was applied to (2) and (3). The gain $(2/t)$ was multiplied to the integration results to obtain even and odd Fourier coefficients at fundamental frequency that are a_1 and b_1, respectively. Signal amplitude was achieved by applying a_1 and b_1 to an equation, $\sqrt{a_1^2 + b_1^2}$. This technique is well-known as "Harmonic analysis base on Fourier transform."

Due to the noisy signal, the suitable number of samples of captured signal, m, (in unit of cycles) was required for obtaining the less noise signal after applying the Fourier transform. Fig. 5 shows calculation output obtained from the simulation and test results when the noise in units of decibels (dB), noise amplitude per one unit of fundamental amplitude, was added to the fundamental signal. The test results also agree with the simulation results. To obtain less noise, a large number of samples of captured signal m was required for the calculation.

The effect of a number of samples of captured signals and scanning speeds were studied. In Figs. 6(a) or 7(a), conductor disconnection ranging from 50 to 500 μm were allocated on the PCB model with conductor width of 200 μm. When the lock-in amplifier was used as a measurement of the ECT signal detected from the SV-GMR sensor, scanning speed and time constant τ was set at 0.001 m/s and 100 ms, respectively. The measurement results, as shown in Figs. 6(b) or 7(b), were clear and had low noise. Refer to specification SR844 from Standford Research Systems, Inc., lowest time constant τ at 100 μs could be set, and then high noise will appear on the acquired ECT signal. For these conditions, scanning speed could increase a little bit because the steady-state signal will be performed after 500 μs, five times of time constant τ. Therefore, the use of Fourier transform, integration technique, spent shorter acquisition time than that of the lock-in amplifier, low-pass filter.

For high scanning speed, the scanning speed was set at 0.05 m/s. The number of samples of captured signal m were set
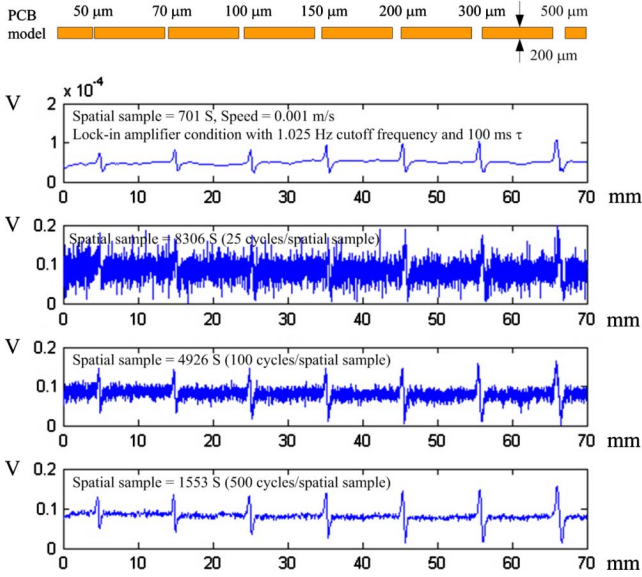
Fig. 6. Effect of the number of samples of captured signal m used to Fourier calculation in application to detect the PCB conductor disconnection. (a) PCB model, (b) ECT signal obtained from lock-in amplifier, and (c)–(e) ECT signal acquired by the proposed technique, at scanning speed of 0.05 m/s, with the number of samples of captured signal, m, of 25, 100, and 500 cycles, respectively.
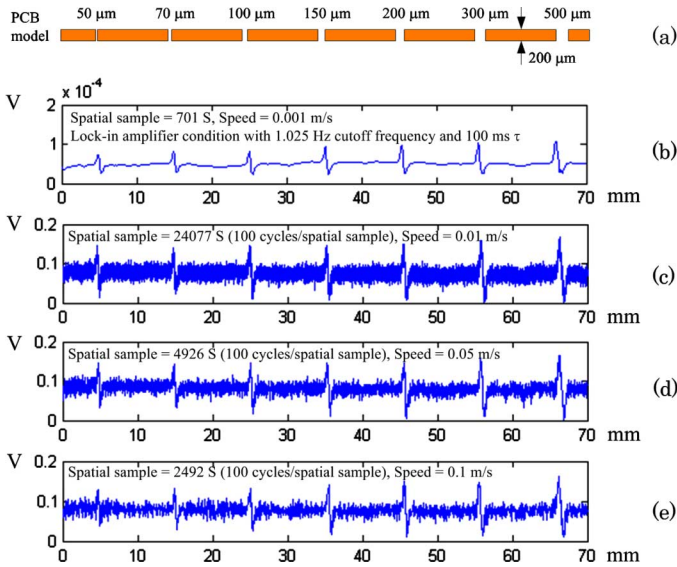

Fig. 7. Effect of scanning speed increasing. (a) PCB model, (b) ECT signal obtained from lock-in amplifier, and (c)–(e) ECT signal acquired by the proposed technique, with the number of samples of captured signal m of 100 cycles, at scanning speed of 0.01, 0.05, and 0.1 m/s, respectively.

to 25, 100, and 500 cycles, and its inspection results are shown in Fig. 6(c)–(e), respectively. The ECT signal acquired with a lesser number of samples of captured signal m provided higher noise than that with a large number of samples of captured signal m. However, an applied simple filtering technique to the signal is possible to enhance the variation of signal at defect point. Furthermore, spatial resolution is high if a lesser number of samples of captured signal is provided.

The sampling data at each point is an average value of signal amplitude at intervals of scanning distance because the probe

keeps continuously moving, while the measurement system also acquires the ECT signal from the SV-GMR sensor. Therefore, the intervals of scanning distance are directly proportional to the scanning speed. This is a cause of the decreasing number of spatial sampling data for the same scanning length when scanning speed is increased. Therefore, the very small defect is difficult to recognize. As shown in Fig. 7(c)–(e), increasing the scanning speed affected the reduction of spatial resolution and the variation of the signal at defect point. Hence, identification of a very small defect is difficult.

The use of harmonic analysis increased the data acquisition rate for a speed up to 10 kS/s depending on the number of samples of captured signal m. Furthermore, the probe was able to scan while the signal was acquired. As a result, the scanning speed could be increased, with less distortion and with higher spatial resolution.

IV. INSPECTION PERFORMANCE

The performance of the proposed PCB inspection system based on ECT technique was tested. A simple PCB model made from Cu with a thickness of 9 μm coated by 0.05 μm Au was used in the experiment. Conductor disconnections ranging from 50 to 500 μm were allocated on the PCB conductor.

Fig. 8 shows SNR versus conductor disconnection when the lock-in amplifier and harmonic analysis were used to acquire the ECT signal from the SV-GMR sensor. By using the lock-in amplifier, the proposed ECT probe was capable of inspecting the PCB conductor disconnection on the 70-μm PCB conductor width, as shown in Fig. 8(a). SNR depends on PCB conductor width and disconnection length. SNR increased gradually as a logarithm function when the PCB conductor width was wider. In contrast, scanning speed was restricted at around 0.001 m/s.

For applied harmonic analysis, SNR dropped depending on the scanning speed and number of samples of captured signal m, as shown in Fig. 8(b) and (c). The probe could inspect the conductor disconnection of 50 μm on 200-μm PCB conductor width and of 100 μm on 100-μm PCB conductor width. For conductor disconnection length that is shorter than 100 μm on the 100-μm PCB conductor width, the signal variation at defect point had almost the same level with noise. Therefore, it is very difficult to identify the SNR exactly. This is because the A/D converter could not acquire the ECT signal at a frequency of 5 MHz without loss, although a high-speed A/D converter was used. However, the scanning speed was faster than that of using the lock-in amplifier and spatial sampling frequency was higher than 10 kS/s depending on the selected number of samples of captured signal m.

Fig. 9 shows 2-D scanning results of a simple PCB model obtained from the high-speed system comparing that from the lock-in amplifier. Defect points on the PCB conductor obviously appeared [Fig. 9(b)] when the lock-in amplifier, with a scanning speed of 0.001 m/s and spatial resolution of 50 S/mm, was used to acquire the ECT signal. For the proposed technique as shown in Fig. 9(c)–(f), a large number of samples of captured signal m used for Fourier calculation, provided clear inspection; however, it provided low spatial
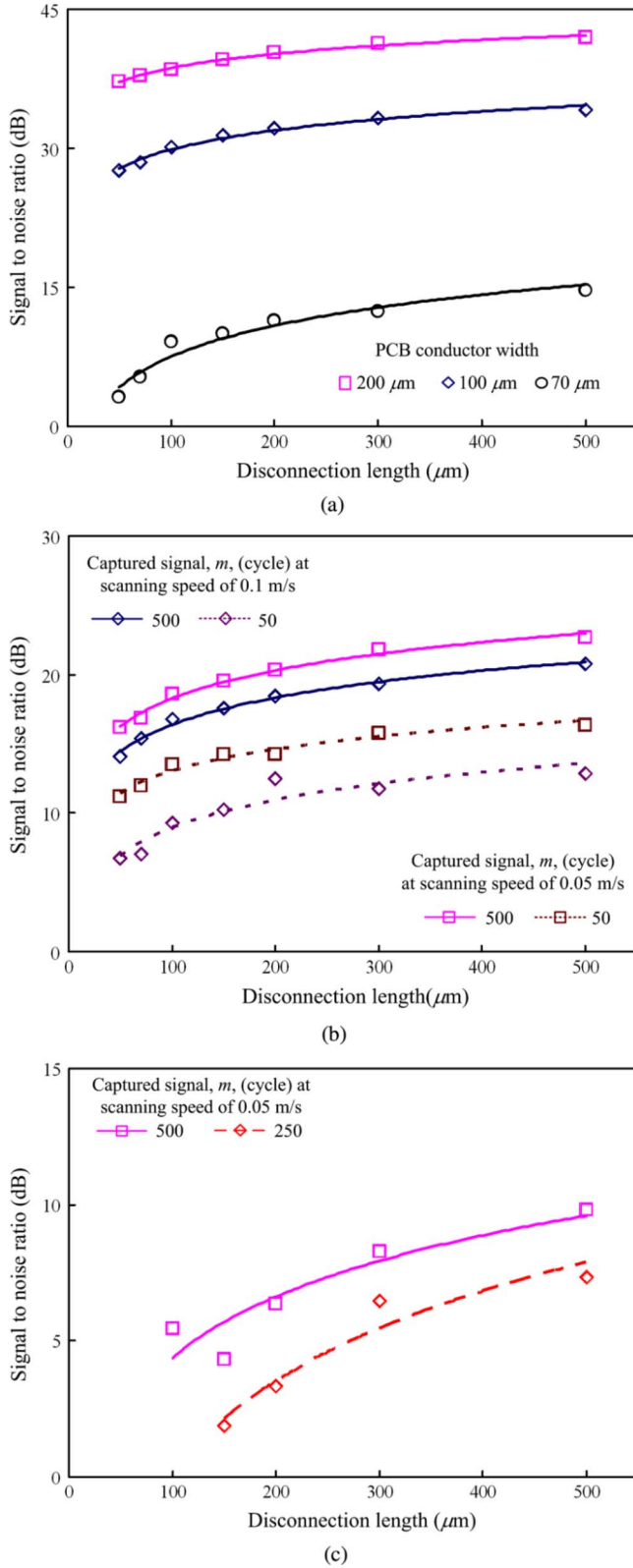
Fig. 8. Signal-to-noise ratio versus disconnection length. (a) Lock-in amplifier is used to measure the amplitude of ECT signal. (b) Harmonic analysis is applied to extract the amplitude of ECT signal for inspection of 200-μm PCB conductor width. (c) Harmonic analysis is applied to extract the amplitude of ECT signal for inspection of 100-μm PCB conductor width.
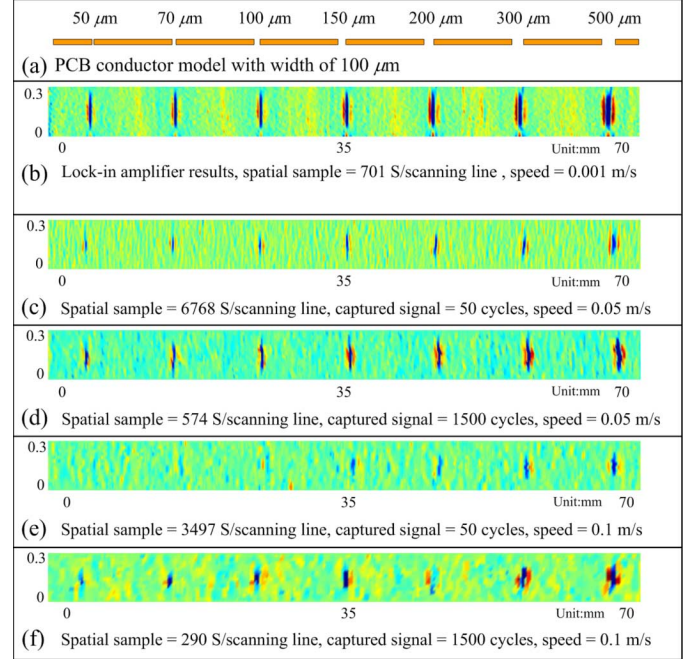

Fig. 9. Scanning results for a simple PCB model with a 100-μm PCB conductor width and conductor disconnection ranging from 50 to 500 μm.

than the higher speed scanning, 0.1 m/s. This is because data acquisition performance was limited by the A/D converter. To obtain an accurate inspection, at least 100 S/mm of scanning resolution was needed even though the higher scanning speed was used. Using 2-D data, 70-μm conductor disconnection length occurred on 100-μm PCB conductor width, which it was able to detect. This is because the simple image processing technique could enhance signal variation at defect point.

To confirm the performance of the proposed technique, the real PCB model was inspected; the PCB model and its inspection results, represented in 2-D image, are shown in Fig. 10. The model size is 10 mm × 5 mm, as shown in Fig. 10(a). Conductor disconnection and partial defects were allocated on the model. The probe scanned the PCB model in the y-direction, with x-direction pitch of 20 μm. Inspection results of nondefect PCB model were used as a reference image. Defect on the tested PCB can be identified based on comparison of the inspection results between the reference and tested PCB.

The tested PCB were scanned at a speed of 0.02 m/s and the results are shown in Fig. 10(b) and (c), and at a speed of 0.05 m/s, the results are shown in Fig. 10(d) and (e). Scanning resolution is 200 and 100 S/mm for a speed of 0.02 and 0.05 m/s, respectively, while scanning finished within 5 min; it is faster than using the lock-in amplifier approximately 30 times. In case of conductor disconnection, the defect points were clearly identified. For partial defect, it is usually difficult to specify because the detected ECT signal is low. However, applying high-performance image enhancement can make it easier to identify the partial defects.

V. CONCLUSION

The ECT probe with the SV-GMR sensor is successfully applied to detect microdefects on a microconductor of a high-

sampling frequency. The lower speed scanning, 0.05 m/s, gave better inspection results and higher spatial sampling frequency
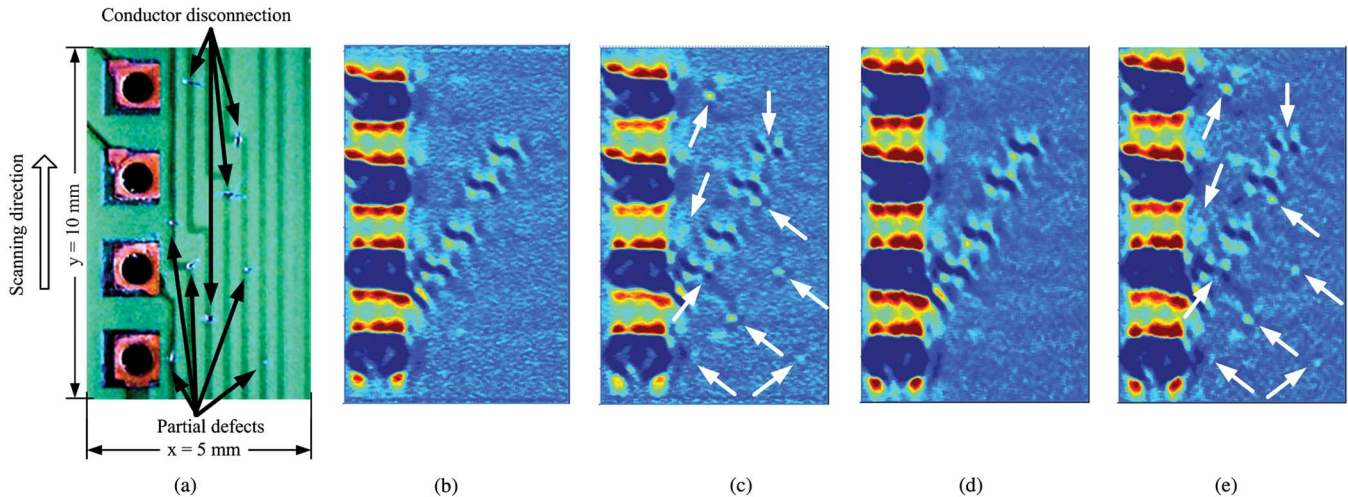
Fig. 10. Photograph of tested PCB model and its inspection results represented in 2-D image. (a) Photograph of bare PCB model. (b) Scanning result of reference PCB model at scanning speed of 0.02 m/s with number of samples of captured signal m of 100 cycles. (c) Scanning result of tested PCB model at scanning speed of 0.02 m/s with number of samples of captured signal m of 100 cycles. (d) Scanning result of reference PCB model at scanning speed of 0.05 m/s with number of samples of captured signal m of 100 cycles. (e) Scanning result of tested PCB model at scanning speed of 0.05 m/s with number of samples of captured signal m of 100 cycles.

density bare PCB. Applied harmonic analysis based on Fourier transform was able to decrease the inspection time. By the proposed technique, high-inspection throughput and high-spatial resolution inspection could be obtained, but the inspection performance was decreased. To obtain a higher performance inspection, a noise reduction had to be applied to the ECT signal before feeding it to the harmonic analysis part.

REFERENCES

[1] M. Moganti and F. Ercal, "Automatic PCB inspection systems," *IEEE Potentials*, vol. 14, no. 3, pp. 6–10, Aug.–Sep. 1995.

[2] T. Dogaru, C. H. Smith, R. W. Schneider, and S. T. Smith, "Deep crack detection around fastener holes in airplane multi-layered structures using GMR-based eddy current probes," *Review of Progress in QNDE*, vol. 23, pp. 398–405, 2004.

[3] R. Grimberg, L. Udpa, S. Udpa, and A. Savin, "A novel rotating magnetic field eddy current transducer for the examination of fuel channels in PHWR nuclear power plants," *Review of Progress in QNDE*, vol. 24, pp. 471–478, 2005.

[4] S. Yamada, K. Chomsuwan, Y. Fukuda, M. Iwahara, H. Wakiwaka, and S. Shoji, "Eddy-current testing probe with spin-valve type GMR sensor for printed circuit board inspection," *IEEE Trans. Magn.*, vol. 40, no. 4, pp. 2676–2678, Jul 2004.

[5] K. Chomsuwan, S. Yamada, M. Iwahara, H. Wakiwaka, and S. Shoji, "Application of eddy-current testing technique for high-density double-layer printed circuit board inspection," *IEEE Trans. Magn.*, vol. 41, no. 10, pp. 3619–3621, Oct. 2005.

[6] S. Yamada, K. Chomsuwan, M. Iwahara, H. Wakiwaka, and S. Shoji, "PCB conductor dimension and alignment inspection with GMR based ECT probe," *Review of Progress in QNDE*, vol. 24, pp. 479–486, 2005.

[7] J. Lenz and S. Edelstein, "Magnetic sensors and their applications," *IEEE Sensors J.*, vol. 6, no. 3, pp. 631–649, Jun. 2006.

[8] S. C. Mukhopadhyay, "A novel planar mesh-type microelectromagnetic sensor—Part I: Model formulation," *IEEE Sensors J.*, vol. 4, no. 3, pp. 301–307, Jun. 2004.

[9] S. C. Mukhopadhyay, "A novel planar mesh-type microelectromagnetic sensor—Part II: Estimation of system properties," *IEEE Sensors J.*, vol. 4, no. 3, pp. 308–312, Jun. 2004.

[10] T. Dogaru and S. T. Smith, "Giant magnetoresistance-based eddy-current sensor," *IEEE Trans. Magn.*, vol. 37, no. 5, pp. 3831–3838, Sep. 2001.

[11] User's Manual Model SR844 RF Lock-in Amplifier Standford Research Systems, Inc., Sunnyvale, CA, 1997, Rev. 2.5.

[12] G. Lafontaine, "Eddy current array probes for faster, better and cheaper inspections," *e-Journal NDT* vol. 5, no. 10, Oct. 2000. [Online]. Available: http://www.ndt.net/article/v05n10/lafont1/lafont1.htm

[13] S. Yamada, K. Nakamura, M. Iwahara, T. Taniguchi, and H. Wakiwaka, "Application of ECT technique for inspection of bare PCB," *IEEE Trans. Magn.*, vol. 39, no. 5, pp. 3325–3327, Sep. 2003.
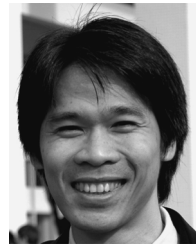
Komkrit Chomsuwan (M'05) was born in Bangkok, Thailand, in 1974. He graduated from the Department of Electrical Technology Education, King Mongkut's Institute of Technology, Thonburi, Bangkok, Thailand, in 1995. He received the M.Eng. degree in electrical engineering from King Mongkut's Institute of Technology, Ladkrabang, Bangkok, Thailand, in 2002, and the Ph.D. degree in engineering from Kanazawa University, Kanazawa, Japan, in 2005.

From 1996 to 1999, he was with the Department of Electrical Technology Education, King Mongkut's Institute of Technology Thonburi, as a Lecturer. Since 1999, he has been with the Department of Electrical Technology Education, King Mongkut's University of Technology Thonburi. He was also with the Kanazawa University as a Researcher and Doctoral Student until March 2006. His research interests include electromagnetics, nondestructive testing, electrical machines, power electronics, and control.

Dr. Chomsuwan is a member of the Institute of Electrical Engineering of Japan and the Magnetics Society of Japan. In 2002, he received the Monbukagakusho Fellowship from Japan. In March 2006, he received a one-year Postdoctoral Researcher Fellowship from the Institute of Nature and Environmental Technology, Kanazawa University.

Sotoshi Yamada (M'86) was born in Kanazawa, Japan, on November 22, 1949. He received the B.E. and M.E. degrees from the Department of Electrical Engineering, Kanazawa University, Kanazawa, Japan, in 1972 and 1974, respectively, and the D.Eng. degree from Kyushu University, Fukuoka, Japan, in 1995.

From 1974 to 1992, he has been with the Department of Electrical and Computer Engineering, Faculty of Engineering, Kanazawa University. He was a Professor at the Laboratory of Magnetic Field Control and Applications from 1992 to 2001. He has been with the Institute of Nature and Environmental Technology, Kanazawa University since 2002. He has been engaged in research on nondestructive testing by giant-magnetoresistance sensor, power magnetic devices, numerical electromagnetic field calculation, biomagnetics, and etc.

Prof. Yamada is a member of the Institute of Electrical Engineering of Japan and the Magnetics Society of Japan.

Masayoshi Iwahara (M'74) received the B.A. and B.S. degree from Fukui University, Fukui, Japan, in 1966, and the Ph.D. degree in the electrical engineering from Kyushu University, Fukuoka, Japan, in 1992.

Currently, he is a Professor at the Graduate School of Natural Science and Technology, Kanazawa University, Kanazawa, Japan, where he heads the Smart Electrical Machines Group. His research activities span all facets of electromagnetic devices and equipment with particular emphasis on nonlinear applied magnetics and numerical analysis methods concerning with electromagnetic mechanical coupling system in time domain.

Prof. Iwahara is the Head of the Hokuriku Branch of the Institution of Electrical Engineers, Japan.